Importance of Mesoscale Features in the Gulf of Mexico on Larval Pelagic Fish Abundance

S Habtes[1], MA Roffer[2], JT Lamkin[3], F Muller-Karger[1], D Lindo[4], BA Muhling[4], M Upton[2], G Gawlikowski[2]

This work is used to aid in the development of spawning site habitat classification and catchability indices of larvae developed from remotely sensed satellite data, in order to *reduce the variance* in the estimates of adult Atlantic bluefin tuna indices of larvae spawning stock abundance in the Gulf of Mexico

Introduction

The management of fisheries requires accurate estimates of spawning stock biomass, preferably through use of accurate fishery independent indices. Better understanding of environmental variables that affect larvae distribution in the Gulf of Mexico will help improve fisheries-related indices. We studied whether larvae catch during annual NOAA surveys were related to mesoscale circulation features. Visual and automated methods of classifying the features were compared. Variability in larval abundances and species diversity was assessed using non-parametric MANOVA and distance-based Canonical Discriminant Analysis (db-CDA).

Methods

Larval abundances (number of larvae per m^3) collected in the Gulf of Mexico during the NOAA SEAMAP (Southeast Area Mapping and Assessment Program) Spring Ichthyoplankton survey (April-June 1993-2007) [1] were compared with sea surface height (SSH) maps obtained from satellite altimeters [2, 3]). Surface Current Velocity (SCV) was obtained from AVISO, and were derived using the Rio model.

Mesoscale features were characterized as cyclonic or anticyclonic regions, cyclonic or anticyclonic boundaries, or Gulf of Mexico 'common water' based on the analysis of SSH and the SSH gradient or grad(*SSH*) values:

- an anticyclonic region (AR) when:
  $$SSH > SSH_{max} - n \cdot \sigma(SSH)$$
- a cyclonic region (CR) when:
  $$SSH \leq SSH_{min} + p \cdot \sigma(SSH)$$
- an anticyclonic boundary (AB) when:
  $$SSH \geq m \cdot SSH_{max} \quad \text{and} \quad \text{grad}(SSH) \geq r \cdot \sigma(\text{grad}(SSH))$$
- a cyclonic boundary (CB) when:
  $$SSH \leq q \cdot SSH_{min} \quad \text{and} \quad \text{grad}(SSH) \geq r \cdot \sigma(\text{grad}(SSH))$$
- or common waters (CW) if none of these conditions are satisfied

with $m = 0.91$; $n = 3.30$; $p = 0.60$; $q = 1.08$ and $r = 0.67$ (optimized for better results).

Also, seven day means of Sea Surface Temperature (SST) obtained from Advanced Very High Resolution Radiometer (AVHRR) and chlorophyll_a (CHL) from the Moderate Resolution Imaging Spectroradiometer (MODIS) and Sea-viewing Wide Field-of-view Sensor (SeaWiFS) were overlaid with contours of AVISO sea height anomaly (SSHA) ¼ degree gridded data products for the survey sampling periods(Fig. 1). Station locations were plotted on the combined altimetry and SST or CHL image and used to determine mesoscale features by visual inspection.

Visual classification of features was necessary because the automated feature classification algorithm was not able to differentiate between Anticyclonic Regions (AR) and the Loop Current (LC) and Loop Current Boundary (LBO). The higher spatial resolution (7 km) of the SST and CHL products allowed the resolution of finer scale processes sometimes missed by the altimeter data (Fig. 1). Boundaries of features were determined by fronts in SST or CHL_a completely surrounding a feature.

Mean abundances of larvae for each mesoscale feature class was standardized by total numbers sampled for all larvae captured in that feature class. A non-parametric pairwise Manova and distance based-Canonical Discriminant Analysis was then used.

Results

Automated assessment of larval abundances using algorithms to determine mesoscale features found higher numbers of larvae of bluefin tuna, bullet/frigate tuna, and little tunny associated with anticyclonic boundaries and common water. Blackfin/yellowfin tuna and dolphinfish abundances had a broader spatial distribution and were not associated with any clear feature class (Fig. 3).

The visual classification indicated that more bluefin tuna and dolphinfish larvae were associated with anticyclonic regions. Little tunny were more closely associated with anticyclonic boundaries. Bullet/frigate tuna and blackfin/yellowfin had a broader distribution with slightly higher abundances along the Loop Current Boundary (Fig. 3).

7-day Chl_a and SST Means with Altimetry Contours

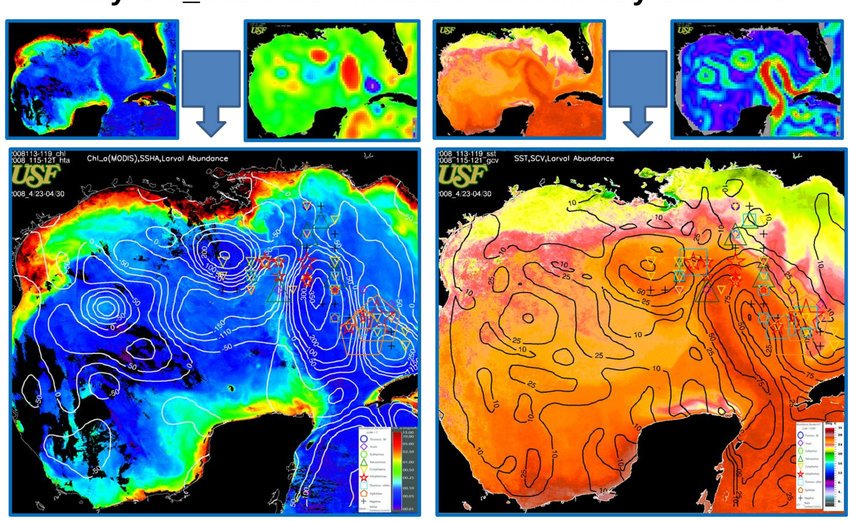

Figure 1. Process for the creation of data products from remotely sensed sst, chl_a, and AVISO altimetry products. From left to right 7-day means of chl_a, ssha, sst, and scv. Bottom left and right: compiled overlays of ssha and chl_a and sst and scv, respectively.

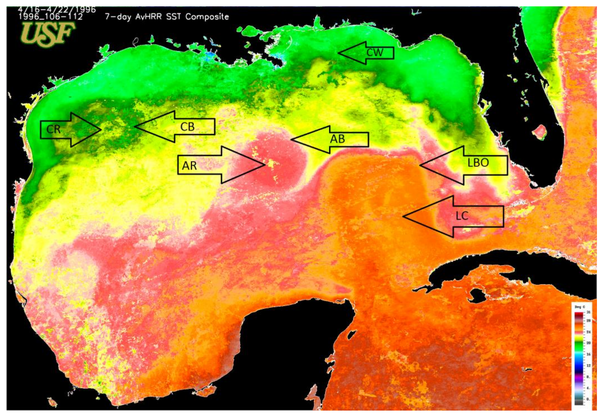

Figure 2. 7 day Mean SST image with mesoscale featrue classifications illustrated. Common water (CW), Loop Current (LC), cyclonic boundary (CB), Loop Current Boundary (LBO), cyclonic region (CR), anticyclonic boundary (AB), anticyclonic region (AR)

Standardized Mean Abundance of Larvae in Mesoscale Features

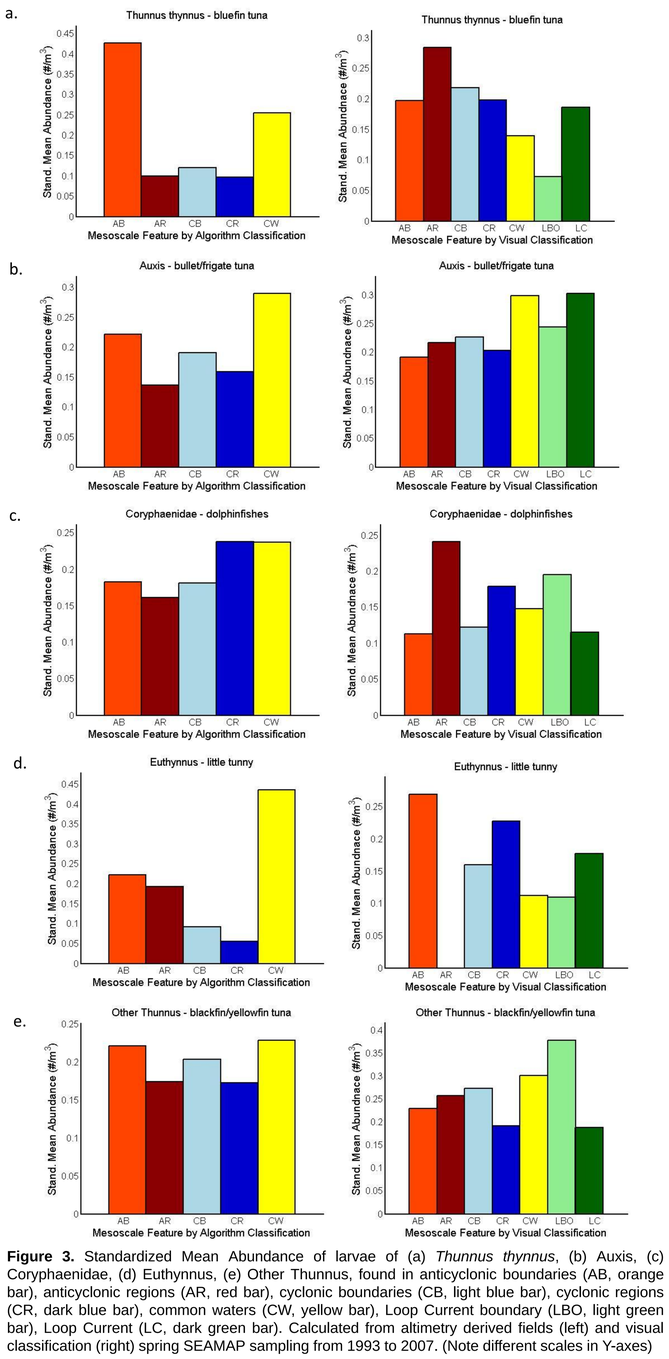

Figure 3. Standardized Mean Abundance of larvae of (a) *Thunnus thynnus*, (b) Auxis, (c) Coryphaenidae, (d) Euthynnus, (e) Other Thunnus, found in anticyclonic boundaries (AB, orange bar), anticyclonic regions (AR, red bar), cyclonic boundaries (CB, light blue bar), cyclonic regions (CR, dark blue bar), common waters (CW, yellow bar), Loop Current boundary (LBO, light green bar), Loop Current (LC, dark green bar). Calculated from altimetry derived fields (left) and visual classification (right) spring SEAMAP sampling from 1993 to 2007. (Note different scales in Y-axes)

Db-CDA and Ordination Bi-plot of Larval Abundance and Mesoscale Features

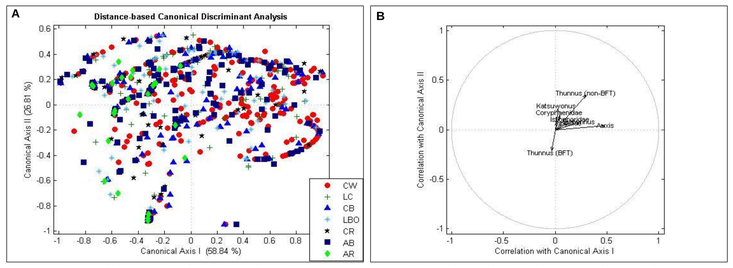

Figure 4. A: Canonical Discriminant Analysis of mesoscale features, this plot shows the relationship of mesoscale features with the variance in larval abundance associated in the first two axis of the CDA, common water (CW, red circle), Loop Current (LC, green plus sign), cyclonic boundaries (CB, blue triangle), Loop Current Boundary (LBO, blue asterisk), cyclonic region (CR, black star), anticyclonic boundaries (AB, blue square), anticyclonic regions (AR, green diamond). **B:** Ordination bi-plot of *Thunnus thynnus* –Thunnus (BFT), Auxis , Coryphaenidae, Euthynnus , Other Thunnus – Thunnus (non-BFT).

These differences maybe attributed to the decreased detail of classification yielded by the automated classification of mesoscale features and the larger spatial range given to the category of anticyclonic boundaries by the automated classification, both possibly inflating the abundances within specific feature classes.

To test how strongly associated with each class of mesoscale features an individual species of larvae was, a non-parametric-Manova and distance based Canonical Discriminant Analysis was used.

Given an alpha level of 0.05 and a p-value of $1x10^{-3}$ of the np-Manova, we can reject the null hypothesis that there are no significant differences in larval abundance and composition associated with mesoscale features. There are differences in larval abundances and compositions based on mesoscale features.

Sample sizes are small in this data set, due to low catch rates associated with this type of sampling. Higher abundances, and numbers of stations with positive larval abundances would have made the test more powerful allowing us a greater ability to detect differences when they exist. There is a slightly significant relationship between the response and predictor variables, with mesoscale features accounting for 75% of the total variation in larval fish abundance and composition.

The CDA plot (Fig. 4A) provides a graphical depiction of the differences in mesoscale features associated with the variances in larval abundance along the first two canonical axes. The ordination biplot diagram (Fig. 4B) provides an overall summary of the multivariate relationships between the response variables (larval fish abundance) and the predictor variables (mesoscale features). The relative locations and distances among larval fish groups plotted in the diagram reflect those differences in larval abundance explained by mesoscale features, with cartesian distance on the plot proportional to differences in abundance.

Abundance of bluefin tuna have higher association along canonical axis I (Fig. 4B). The length of each vector is proportional to the strength (magnitude) of the underlying gradient of each variable. However, since Canonical Axis I contributes the most to the "percent variation explained", the distribution of mesoscale feature classes for abundances that are parallel to that axis (or have a significant component along that axis) (Fig. 4A) are deemed more important than those that do not. Anticyclonic regions therefore show more importance in determining regions of higher abundance of bluefin tuna.

Conclusions

Position and strength of mesoscale features in the GOM influence the area and persistence of habitat favorable for larvae distribution. Variability in the formation of eddies in the Gulf of Mexico Loop Current was reflected in larval fish distributions. Each taxa had a different feature class that the highest abundances were associated with. The Canonical Discriminant Analysis (CDA) indicates only bluefin tuna showed a clear relationship to any feature class , anticyclonic regions, and have larval abundances and compositions where bluefin tuna are present very diff

The CDA offers a better method for the analysis of beta diversity in larval fish abundances than ANOSIM or SIMPER analysis which do not correctly partition the variation in the data or give proper type-I error rates [5].

The larval fish distributions in the GOM common waters regions may be investigated in future research by utilizing other indices derived from satellite data.

References

[1] Larval fish data were available from the National Marine Fisheries Service Southeast Area Monitoring and Assessment Program (SEAMAP) database.
[2] Optimally interpolated gridded SHA fields: http://www.aviso.oceanobs.com/en/altimetry/.
[3] Rio MH, F. Hernandez (2004). *A mean dynamic topography computed over the world ocean from altimetry, in situ measurements, and a geoid model*. J Geophys Res Oceans 109:C12032.
[4] Muhling BA, S-K Lee, JT Lamkin, and Y Liu (2011). *Predicting the effects of climate change on bluefin tuna (Thunnus thynnus) spawning habitat in the Gulf of Mexico.* – ICES J Mar Sci 68: 1051–1062.
[5] Anderson, MJ and Willis ,TJ (2003). *Canonical analysis of principal coordinates a useful method of constrained ordination for ecology.* Ecology 84(2):511-525.

[1]University of South Florida - College of Marine Science, [2]Roffer's Ocean Fish Forecasting Service - ROFFS^{TM}, [3]NOAA – Southeast Fisheries Science Center, [4]University of Miami – Cooperative Institute for Marine and Atmospheric Studies (CIMAS)